

EU contract number RII3-CT-2003-506395

CARE-Note-2007-013-ELAN



Strategy to measure the Higgs mass, width and invisible decays at ILC

François Richard, Philip Bambade

Laboratoire de l'Accélérateur Linéaire
IN2P3-CNRS et Université de Paris-Sud XI, Bât. 200, BP 34, 91898 Orsay Cedex
France

PRELIMINARY

LAL-Orsay 07/03
January 2007

Strategy to measure the Higgs mass, width and invisible decays at ILC

François Richard, Philip Bambade

Laboratoire de l'Accélérateur Linéaire
IN2P3-CNRS et Université de Paris-Sud XI, Bât. 200, BP 34, 91898 Orsay Cedex
France

*Work presented at the International Collider Physics and Detector ECFA Workshop
Valencia, Spain, November 7-10 2006*

Abstract

This document is meant to provide semi-quantitative arguments to evaluate the luminosity needed at ILC to achieve a precise measurement of the Higgs mass, width and invisible decays. It is shown that for $m_H=120$ GeV, one can save an order of magnitude on the luminosity needed to achieve a given precision on the Higgs mass, as compared to what can be obtained at $\sqrt{s}=350$ GeV, by running near threshold. Since the recoil mass resolution near threshold is independent of the Higgs mass, one can also access the Higgs width for masses above 170 GeV. This strategy of running just above threshold is also optimal to measure or set upper limits on the Higgs invisible branching ratio. A simplified description of the various experimental mechanisms affecting this type of measurement is presented: detector resolution for leptons and jets, luminosity and beamstrahlung energy dependence, initial and final radiation of the involved leptons.

1. Introduction

ILC can provide a large sample of clean HZ events. It is therefore expected that with this sample and using the recoil mass to the Z, with Z decaying into $\mu^+\mu^-$ or e^+e^- , one can precisely reconstruct the Higgs boson mass, irrespective of its decay modes.

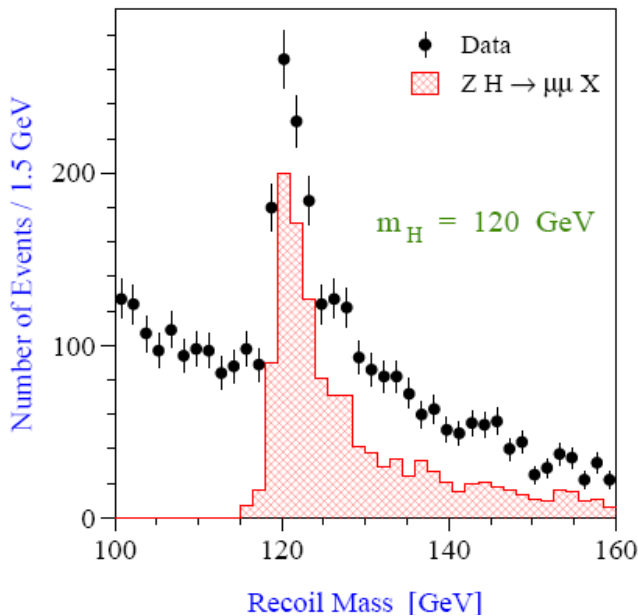


Figure 1: Recoil mass to Z boson for $\sqrt{s} = 350$ GeV [1]

This is illustrated in Figure 1, taken from TESLA TDR [1], where one assumes that the Z decays into muons.

In this note we would like to underline that to achieve the best mass resolution, one needs to operate close to the HZ threshold, contrary to the assumption of previous studies, like the one shown in Figure 1, which suggested using data taken at the top threshold.

Also, improved momentum resolution compared to that assumed in the TESLA TDR can be expected when using the TPC in conjunction with the external detectors (see Figure 6 in the Appendix).

2. Optimal working energy to measure the Higgs mass

We note that the mass resolution of about 1.5 GeV in Figure 1 is obtained at $\sqrt{s}=350$ GeV, which is well above threshold for the considered Higgs mass of 120 GeV. This means that the Z particle is boosted and therefore one finds that the error on the momentum of the muons p , which goes like p^2 , is four times larger on average than near threshold (see Appendix).

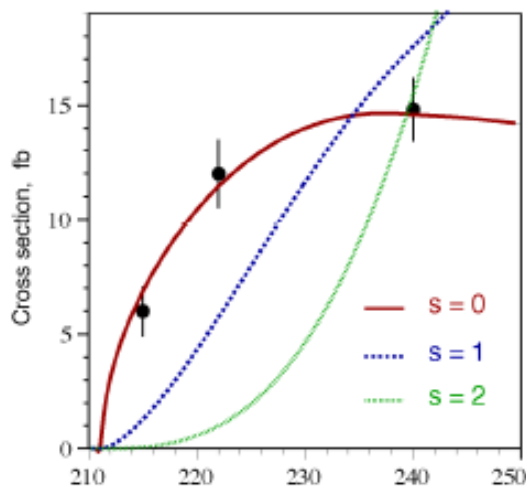


Figure 2: Threshold behaviour of Higgs boson production in association with a Z boson, for different assumptions on its spin [1]

Working near threshold would of course be unattractive if the rate were reduced. However this is not so since HZ is produced in an s-wave and therefore has a steep threshold as shown in Figure 2. Quantitatively, for a 120 GeV Higgs particle, one finds in fact that the production cross section is increased by

about a factor two at 220-230 GeV with respect to its value at 350 GeV [1].

Finally one should note (see Appendix) that similar gains in resolution are obtained using Z hadronic decays, which further justifies operating near threshold.

3. Effect of beamstrahlung

One may object to above arguments that, in spite of an improved mass resolution, the net effect will be significantly attenuated by beamstrahlung (BS). The qualitative reply to this argument can be understood by noticing that, with the TESLA parameters at $\sqrt{s}=500$ GeV, on average more than 50% of the beam particles do not radiate at all before interacting while the rest radiate with strong peaking at small energies. One can therefore expect a mass distribution with a narrow peak reflecting the momentum resolution plus a BS tail carrying about 50% of the cross-section.

To see this, one can use for BS the parameterisation of the beam smearing given in reference [2]:

$$f(x) = a_0\delta(1-x) + a_1x^{a_2}(1-x)^{a_3}$$

with, for $\sqrt{s}=500$ GeV, $a_0=0.53$, $a_2=13.895$ and $a_3=-0.63$ while a_1 is adjusted to get a normalized distribution.

We have instead used the following formula provided by P. Chen and K. Yokoya [3]:

$$g(y) \sim \left[\frac{N_\gamma \kappa^{1/3} e^{-\kappa y}}{\Gamma(1/3) y^{2/3}} + \delta(y) \right] e^{-N_\gamma y}$$

which gives the BS photon distribution when $y=k/E \ll 1$. For ILC (TESLA) at 500 GeV, the total number of emitted photons is $N_\gamma=1.26(1.45)$ while $Y=0.054(0.046)$ and $\kappa=2/(3Y)=14.5(12.3)$. Note that the above formula would give a_0 well below 50%. To get the correct answer one should use the average number of radiated photons emitted before an interaction, which is about one half the total number used above.

The luminosity spectrum was obtained through the formulae in [3] assuming ILC parameters. Good agreement with the generator Guinea Pig [4] was found, as shown in Figure 7 in the Appendix. Using this spectrum and the mass resolution obtained in the Appendix, the differential cross-section for $H\mu\mu$ was computed and is shown in Figure 3, at $\sqrt{s}=230$ GeV (blue curve) and 350 GeV (red curve), strikingly illustrating the improvement expected by running near threshold.

Table 1 below shows how this improvement translates into a gain in the luminosity needed to reach a given accuracy, 30 MeV, on the Higgs mass measurement.

E_{CM}	$\sigma(H\mu\mu)$ fb No ISR	Average lepton momentum, GeV	σ_{Mh} MeV	Muon Radcor	Electron Radcor	$\mathcal{L}(30 \text{ MeV})$ fb ⁻¹ $\mu\mu+ee$
350	4.6	83	900	0.45	0.27	780
230	9.1	54	200	0.36	0.18	20

Table 1 : Comparison of integrated luminosities at $\sqrt{s} = 230$ and 350 GeV needed to reach a 30 MeV precision on the Higgs boson mass. Also shown are the production cross sections and the average single event mass resolutions σ_{Mh} and lepton momenta. Both internal and external radiative effects are taken into account in the evaluation (see Appendix).

Additional considerations

1/ The energy widths of the beams, which are at the $6 \cdot 10^{-4}$ level on average, would produce negligible effects given the single event recoil mass resolutions discussed. The mean beam energy would on the other hand need to be stable from bunch to bunch (or at least monitored) at the level of a $1\text{-}2 \cdot 10^{-4}$ for 350-230 GeV, to avoid degrading the final mass resolution.

2/ Initial (ISR) and final state (FSR) radiation effects must be taken into account in the evaluation. The net effect is to reduce the peak by about $(2.35\sigma_{Mh}/E_{CM})^b$ where b is the equivalent radiator. The value of b is about 11.5% for ISR. For FSR, the value of b is about 6% for muons and 10.7% for electrons. Radiation in the detector can be estimated at the 4% level and also result in a lower efficiency (see Appendix). One

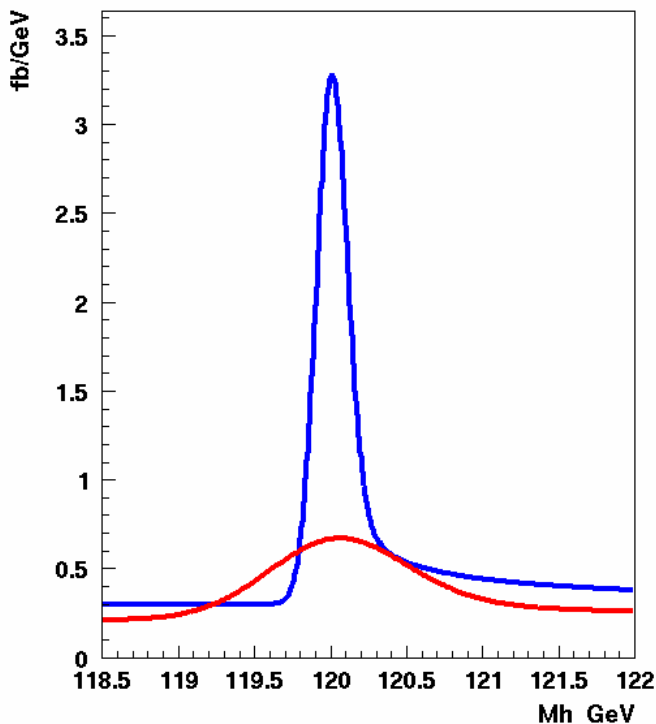


Figure 3: Differential cross-section for $H\mu\mu$ at $\sqrt{s}=230$ GeV (blue curve) and 350 GeV (red curve)

could try to recover partially the loss from FSR by measuring the radiated photons in the ECAL but this can only work for photons below 500 MeV given the poor resolution of ECAL as compared to the tracking.

3/ A 5-constraint kinematic fit, imposing energy-momentum conservation and the Z boson mass, would not help for leptonic decays, given that the resolution on the Z mass $\sim 1/\sqrt{2}\sigma_p/p$ which for $p\sim 45$ GeV and $\sigma_p/p^2=5\cdot 10^{-5}$ GeV $^{-1}$, gives 0.16% or 150 MeV, is well below the Z natural width. This remains true, given the assumed momentum resolution, even if one operates at $\sqrt{s}=500$ GeV. A 4-constraint kinematic fit using only energy-momentum conservation mass resolution but would of course depend on the Higgs boson decay mode.

4. Energy dependence of the Luminosity

Beam parameter optimisation: The evaluation in Table 1 implicitly assumes that the luminosity \mathcal{L} does not depend on energy, which is not necessarily exactly the case. Generally speaking [5], optimising the luminosity of a linear collider in the presence of beam-beam effects leads to:

$$\mathcal{L} \sim \eta \frac{P_{\text{Electrical}}}{E_{CM}} \sqrt{\frac{\delta}{\epsilon_{n,y}}} H_D$$

The effective beam power ηP (or at least its upper limit) and the normalized vertical emittance $\varepsilon_{n,y}$ can be considered fixed parameters for most linear collider designs. In our calculation we have also assumed that the beamstrahlung parameter δ could be maintained constant. This would imply a luminosity which increases at lower energy. In practice this is however not realistic since the number of particles per bunch N usually has an upper limit due to wake-field effects, or is limited within the damping rings. The beam power P is therefore proportional to energy and the overall luminosity constant as long as δ can indeed be maintained constant.

But is it possible to maintain a fixed δ ? This parameter goes like:

$$\delta = E_{CM} \frac{N^2}{\sigma_z \sigma_x^2} \quad \text{with} \quad \sigma_x^2 \sim \varepsilon_x \beta_x / \gamma$$

meaning that for fixed N and ε_x , the product $\beta_x \sigma_z$ should be reduced as the square of E_{CM}^2 . If σ_z is reduced, then one can also consider somewhat increasing the luminosity by reducing β_y by a similar factor. This is so because the above mentioned luminosity optimisation normally assumes $\sigma_z \leq \beta_y$ to avoid optical depth of field effects in the vertical plane at the interaction point (the so-called hour-glass effect).

Using the Guinea Pig simulation we have checked that it is indeed possible to recover the luminosity reachable with nominal parameter at 350 GeV, either by decreasing β_x by about a factor 2 with respect to the nominal value or, alternatively, by simultaneously decreasing β_x and σ_z by a factor 2/3 and β_y by a factor 2.

With such parameters, beamstrahlung emission is maintained constant between 350 and 230 GeV. With the standard parameters, beamstrahlung emission would decrease, however the fraction of the luminosity within an energy bin corresponding to the narrow single-event Higgs boson recoil mass resolution would increase only by about 30% while the total luminosity would decrease by a factor 2. Hence increasing the luminosity by increasing the beamstrahlung is unexpectedly beneficial in this particular instance. Since the gain is moderate, such an optimisation is not absolutely crucial to the running scenario described here, which is also a good sign for the robustness of the results obtained.

While the proposed optimised parameters ($\beta_x \sim 10\text{--}15$ mm, $\sigma_z \sim 0.2\text{--}0.3$ mm and $\beta_y \sim 0.2\text{--}0.4$ mm) are within the range considered for the ILC design, they are close to its edge. Practical feasibility should be explored further. Overall, there seems nonetheless to be enough flexibility to keep similar luminosity at 230 as at 350 GeV, and hence benefit from the larger cross section near threshold.

Undulator-based positron production: The operational scenario suggested in this paper also assumes that one can run at 230 GeV without limitations. This may not be exactly true in the undulator scheme, which uses electrons with at least 150 GeV to generate the positron beam. To be able to run near the Higgs boson production threshold as advocated, the electron beam must be decelerated from 150 GeV to about 115 GeV after its passage through the undulator. This may have practical implications (or even unwanted consequences) and is therefore important to analyse carefully. A solution should be found to enable running with reasonable performance near this limit, or else this could constitute an objection to the undulator idea itself,

given the importance of achieving optimal running conditions for the HZ channel and the need for a threshold scan.

5. Measuring the Higgs boson width?

Much more challenging would be to measure the effect of the Higgs width on the Gaussian mass distribution. Two obvious difficulties are to be considered:

1/ The size of the width itself which, in the SM, is negligible for Higgs boson masses below about 170 GeV,

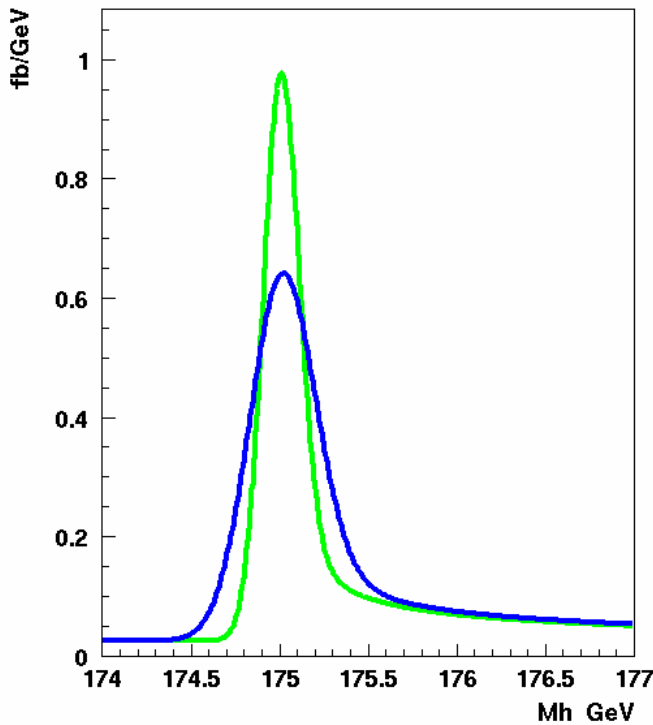


Figure 4 : Differential cross-section for $H\mu\mu$ at $\sqrt{s}=290$ GeV for $M_H=175$ GeV with (blue) and without (green) including the Breit-Wigner width.

2/ The effect of this width on the effective resolution, in case the two should be combined quadratically.

Empirically, one finds however that combining Gaussian and Breit-Wigner distributions with σ° and Γ widths, respectively, results in the following linear dependence for the total width σ of the combined distribution:

$$\sigma = \sigma^\circ + 0.65 * \Gamma / 2$$

The possibility to measure the Higgs width is illustrated in Figure 4 for $\Gamma_H=500$ MeV, corresponding to $M_H=175$ GeV in the Standard Model. The picture compares the distributions obtained combining (blue curve) or not (green curve) the Higgs boson width with the mass distribution.

Table 2 gives the integrated luminosity needed to measure the Higgs boson width to a 10%

accuracy, assuming that σ^0 can be predicted accurately to deduce it from the overall width σ .

ECM GeV	$\sigma(H\mu\mu)$ fb	Average muon momentum, GeV	σ_{Mh} MeV	\mathcal{L} (10%) fb^{-1}
350	3.1	71.5	455	500
290	3.2	53	200	100

Table 2: Comparison of integrated luminosities at $\sqrt{s} = 290$ and 350 GeV needed to reach a 10% accuracy on the SM Higgs boson width, for $M_H=175$ GeV. Also shown are the production cross sections and the average single event mass resolutions σ_{Mh} and lepton momenta.

It is remarkable that the recoil mass resolution at threshold does not increase with Higgs boson mass. This means that if such a heavy Higgs is produced at ILC, there is some hope to measure its width.

It should be noted that for such a measurement to be feasible, both the momentum resolution of the final state leptons and the differential luminosity spectrum must be known accurately. Running at the Z pole, where muon pairs are mono-energetic, allows a direct verification of the momentum resolution and also an absolute calibration of the momentum in the appropriate range. Concerning the luminosity spectrum, it can be precisely monitored using the acollinearity distribution [7] of Bhabha events.

6. An MSSM scenario

Within the Minimal Super Symmetrical Model (MSSM) the lightest Higgs boson has a mass of about 120 GeV and, in what is called the decoupling scenario, where the pseudo-scalar Higgs A is very heavy, behaves like the Standard Model Higgs, which means that its width is not measurable. There is however another possible scenario in which the two CP-even Higgs states, h and H, are almost degenerate in mass with A and can be observed simultaneously in the hZ and HZ channels. Moreover the couplings to b quarks can be at variance with the Standard Model prediction when $\tan\beta$ becomes very large, thereby increasing the total width to a measurable value. Reference [6] proposes such a scenario, the main parameters of which are summarised in Table 3.

Type	σ_{hZ}/SM	Γ_{tot} GeV	Mass GeV
h	0.873	0.18	123
H	0.127	0.873	136

Table 3: Main parameters of the MSSM scenario described in [6].

Figure 5 shows the expected behaviour of the reconstruction of the h and H Higgs boson masses in this model, at $E_{cm}=230$ GeV (blue curve) and at $E_{cm}=350$ GeV (red curve), illustrating both the potential of ILC in this scenario and the improvement expected at 230 GeV. Note that we assume that the $ZZ\gamma$ background can be removed by measuring the b-quark pair decays of the two Higgs particles, which represent about 90% of the branching ratios.

In this scenario, ILC can:

- 1/ Separate the two states and therefore measure the masses M_h and M_H and the couplings, which allows $\sin^2(\alpha-\beta)$ to be determined,
- 2/ Measure the widths, which provide the two quantities $\sin^2\alpha/\cos^2\beta$ and $\cos^2\alpha/\cos^2\beta$.

These six observables, where α and β are mixing angles, over-constrain the MSSM and allow a complete verification of this model. Deviations from MSSM predictions would establish some mixing effects with a non-minimal component, usually an

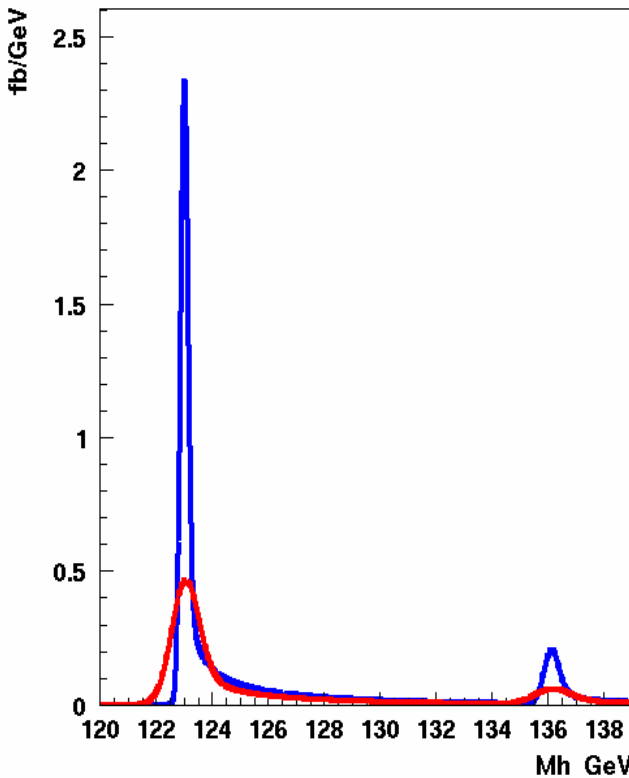


Figure 5: Differential cross-section for $h\mu\mu$ and $H\mu\mu$ in the MSSM model described in [6], at $\sqrt{s}=230$ GeV (blue) and $\sqrt{s}=350$ GeV (red)

best example being the lepton number violation related to neutrino masses (e.g. the Majorons).

Since a light Higgs boson mass, say below 150 GeV, couples very weakly to standard fermions (hence the very narrow width expected) there is a definite possibility that these new particles could significantly contribute to, or eventually entirely dominate, the Higgs particle decays. It is therefore essential to provide the highest sensitivity on the measurement on the Higgs invisible branching ratio BR_{inv} , as it carries a large discovery potential.

LHC can reach a 5 % (13%) limit on BR_{inv} with 100 fb^{-1} (10 fb^{-1}) [8]. This may or may not be sufficient to see the manifestation of such models.

To understand the role of mass resolution, signal and background contributions one can write the significance of a signal as:

$$\frac{N_{Sig}}{\sqrt{N_{Bg}}} = \sqrt{\frac{L}{n\sigma_{Mh}}} \frac{BR_{inv}\epsilon_{HZ}\sigma_{HZ}}{\sqrt{\epsilon_{ZZ}\sigma_{ZZ}}}$$

This formula says that the luminosity L needed increases proportionally to the mass resolution and decreases quadratically with the HZ cross-section. The latter means that the hadronic Z decays provide the highest sensitivity. Taking a mass interval $\pm 2\sigma_{Mh}$ corresponds to $n=4$ in our formula. The results from [9] can then be easily reproduced with this expression with $\sigma_{Mh}=7.3$ GeV and $\epsilon_{HZ}=34\%$, which seems reasonable taking into account ISR and beamstrahlung effects.

The advantage of operating at 230 GeV rather than 350 GeV in the centre-of-mass is illustrated in Table 4. The semi-analytical evaluation of the single event recoil mass

isoscalar Higgs boson, or eventually other types of scalar like radions, as predicted within theories with extra dimensions.

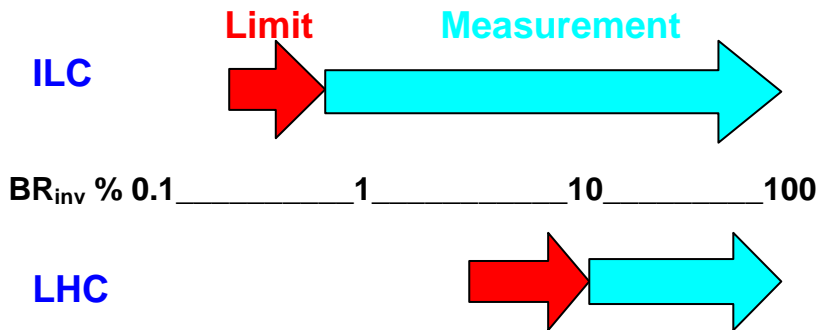
7. Measuring the Higgs invisible decays

In several extensions of the Standard Model one predicts stable neutral light objects. The well known example is the case of the lightest neutralino which is expected to provide a good candidate for dark matter within supersymmetry. There are however many other examples of such particles, for instance in theories with extra dimensions or in other alternate scenarios like the Little Higgs scheme. One can also mention the so-called Goldstone particles, which appear in the context of symmetry violation, the

resolution presented in the Appendix was used. The contribution from the WW final states was neglected (it has been confirmed to be small [9]). Confusion with the standard HZ process when the Z boson decays into neutrinos is assumed to be negligible for a 120 GeV mass as long as an optimal energy flow can be used.

E_{cm} GeV	$\sigma(HZ_{had})$ fb (34% eff)	$\sigma(Z_{had}Z_{inv}+\gamma)$ fb $\pm 2\sigma_{Mh}$	σ_{Mh} GeV Hadrons	\mathcal{L} fb ⁻¹ 95% CL $BR_{inv} < 2\%$ fb ⁻¹	\mathcal{L} fb ⁻¹ measure $BR_{inv} = 2 \pm 0.5\%$
350	30	10	7.3 (1C fit)	85	500
230	60	4	2.3 (1C fit)	8	50

Table 4 : Integrated luminosities at $\sqrt{s} = 230$ and 350 GeV needed to set a 2% upper limit on BR_{inv} at 95% CL and to measure a 2% value with a 0.5% precision, for $M_H=120$ GeV. Also shown are the effective production cross sections in the hadronic mode for a 34% experimental acceptance and the average single event mass resolutions σ_{Mh} .



It should also be stressed that:

- 1/ The mass of an invisibly decaying Higgs (and eventually its width) can also be precisely measured at ILC, which would not be the case at LHC,
- 2/ A branching ratio into fermions remains measurable at ILC down to a fraction of per cent. In this case, the Higgs boson width increases by two orders of magnitude and becomes also measurable even for $m_H=120$ GeV.

If the Higgs boson decays invisibly, but not dominantly ($BR_{inv} < 99\%$), then one can estimate the invisible width due to new physics by comparing it to Standard Model visible decay branching ratio BR_{vis} . If the Higgs decays 100% invisibly, measuring the total width, which would be possible at ILC even for a 120 GeV mass, provides the only observable giving access to an estimate of the Higgs coupling to the invisible particles, an essential piece of information to understand the mechanism.

There are various experimental limitations, especially for very low BR_{inv} values, which come into this analysis but we think that they can be handled using the data themselves. They can of course be studied in Monte Carlo analyses. Examples are: the recoil mass resolution, the background level. Both of these can be monitored using the large sample of ZZ data itself. The same should be true for minor backgrounds like WW and HZ itself.

2/ ISR and FSR can be simply described through the probability distribution:

$$dP = b \frac{dx}{x^{1-b}}$$

where $x=k/E$ is the ratio between the photon and the lepton energies and:

$$b = \frac{2\alpha}{\pi} [\log(\frac{M^2}{m^2}) - 1]$$

where m is the lepton mass and M is the lepton pair mass. For ISR one has simply $M^2=s$ and m is the electron mass. For FSR $M=M_Z$. Remarkably enough one cannot neglect muon FSR, for which $b=5.8\%$, with respect to electron FSR, for which $b=10.8\%$.

3/ External radiation is only relevant for electrons and is governed by the detector properties. For the purpose of this study we have assumed that an electron will see, on average, $d=3\%$ of X^0 before entering the TPC. We have then added this contribution to the FSR for the electrons, taking $b=2(4d/3X^0) = 8\%$ to account for both leptons. This figure shows that the detector properties amplify significantly the losses due to FSR. The net result, shown in Table 1, is a reduction in efficiency of a factor of about two for electrons with respect to muons.

In practice one should convolute the Gaussian (or Breit Wigner) shape of the mass resolution with the probability distribution. This gives for the radiation effect the following attenuation on the peak:

$$P = \left(\frac{\Gamma}{M}\right)^b = \left(\frac{2.35\sigma}{M}\right)^b$$

where $M=E_{cm}$ for ISR and $M=M_Z$ for FSR. This formula can be intuitively derived by integrating the probability distribution given above between 0 and $\Gamma/2$.

The $ZZ\gamma$ background

The ZZ process dominates the background to the HZ channel if one uses the recoil mass method with lepton pairs. In the absence of radiation, only ZZ^* can contaminate HZ with $M_{Z^*}=M_H$. This contribution is however typically one order of magnitude below the contribution from $ZZ\gamma$, where the photon comes either from ISR or from beamstrahlung. This process constitutes a significant background when the energy of this photon is such that one of the Z boson combinations peaks at the Higgs boson mass.

The various components of the ZZ background, for the two energies discussed in the paper, are given in Table 5. For what concerns this background one sees that reducing further the beamstrahlung would not help much near threshold.

Energy GeV	$ZZ^*(120)$	$ZZ\gamma$ RC	$ZZ\gamma$ BS	Sum fb/GeV
230	1	6.7	0.2	7.9
350	0.7	3.1	2.1	5.9

Table 5: Expected backgrounds for $HZ(120 \text{ GeV})$, in fb/GeV, coming from the ZZ process, at the two energies. The $ZZ^*(120)$ background gives a virtual Z at 120 GeV. In the other two processes there is a photon (from initial radiation or beamstrahlung) emitted in the beam pipe with two Z bosons on mass-shell such that the recoil mass to the Z decaying leptonically peaks at 120 GeV.

In most cases an exploration for new physics would require the highest luminosity being taken at $\sqrt{s}=500$ GeV. This is also true for important Standard Model measurements such as $t\bar{t}H$ and ZHH .

It appears however that such an energy does not provide appropriate conditions for studying ZH . Therefore, if LHC confirms the existence of a light Higgs, it will be essential to provide the possibility to run ILC at energies below $\sqrt{s}=300$ GeV with an optimal luminosity.

In the future one needs to perform a complete simulation of the Higgs channels at 230 GeV using the complete tools becoming available. It will also be important to investigate further the energy dependence of the luminosity (see Section 4), in particular to assess the feasibility of the suggested optimised beam parameters and of running below the energy required to produce positrons in the context of the undulator scheme.

Acknowledgements

Useful discussions with K. Moenig are gratefully acknowledged. We also wish to thank Y. Mambrini and M. Berggren for providing, respectively, the detailed parameters of the MSSM study and an updated momentum resolution curve from the LDC concept study

We acknowledge the support of the European Community-Research Infrastructure Activity under the FP6 "Structuring the European Research Area" programme (CARE, contract number RII3-CT-2003-506395)

References

- [1] TESLA Technical Design Report Part III: Physics at an e^+e^- Linear Collider, hep-ph/0106315.
For a more recent analysis, see P. Garcia-Abia, W. Lohmann, A. Raspereza, in Eur.Phys.J.C44:481-488,2005.
- [2] K. Moenig, LC-PHSM-2000-60-TESLA.
- [3] K. Yokoya, P. Chen in Proceedings, Accelerator science and technology, (IEEE, 1989).
- [4] Guinea Pig, see <https://trac.lal.in2p3.fr/GuineaPig>.
- [5] D. Schulte, PhD Thesis, University of Hamburg 1996.
- [6] A. Djouadi and Y. Mambrini Sept 2006, hep-ph/0609234.
- [7] K. Moenig, LC-PHSM-2000-060, Dec 2000.
In "2nd ECFA/DESY Study 1998-2001" 1353-1361.
M. Frary and D. Miller, DESY 92-123A.
- [8] O.J.P. Eboli, D. Zeppenfeld, Phys.Lett.B495:147-154,2000.
- [9] M. Schumacher, LC-PHSM-2003-096, Nov 2003.
- [10] M. Berggren, Work presented at the International Collider Physics and Detector ECFA Workshop Valencia, Spain, November 7-10 2006 and private communication (see <http://ific.uv.es/~ilc/ECFA-GDE2006/>).
- [11] Detector Concept Report for the ILC, Editors T. Behnke, C. Damerell, J. Jaros, A. Miyamoto, <http://www.desy.de/~behnke/dcr/Detector/DCR.pdf>

Appendix

Mass resolution

1/ For leptonic decays of the Z boson, and taking that $\sigma_p/p^2=k$ ($k=5 \cdot 10^{-5} \text{ GeV}^{-1}$ for the TESLA design), one easily derives the recoil mass error to the Z in the HZ mode:

$$\delta M_h^2 = \sqrt{2kp(4Ep - M_Z^2)}$$

where, near threshold, $2E \sim M_H + M_Z$ and the lepton momentum $p \sim M_Z/2$. On the other hand, rather quickly above threshold, $p \sim E/2$ where E is the beam energy and there is a fast deterioration of the mass resolution.

Instead of taking k constant one can use results recently obtained for the LDC [10] detector concept, which take into account the improved accuracies expected from the TPC and the impact of external silicon detectors. The angular dependence of this momentum resolution is not important and therefore has been neglected here.

One has:

$$p = \frac{4E^2 - M_h^2 + M_Z^2}{8E}$$

which for $2E=230(350) \text{ GeV}$ gives a lepton momentum of $54(83) \text{ GeV}$ for symmetric decays. From the above expression of the mass resolution, one therefore expects a substantial deterioration by going to 350 GeV. For asymmetric decays, this deterioration gets even worse, as it becomes dominated by the most energetic lepton:

$$\delta M_h^2 = kp(4Ep - M_Z^2)$$

The ratio p_{\max}/p varies between 1 and $1+\beta_Z \cos\theta$, where $\beta_Z = 0.39(0.84)$ at 230(350) GeV. Keeping 70% of the events one finds that the mass resolution is increased by up to 80% at 350 GeV. In the results in Tables 1,2 and 4 we have given averaged resolutions with no restriction at 230 GeV and keeping only 70% of the acceptance at 350 GeV. These averaged resolutions have significant dispersions: $200 \pm 30 \text{ MeV}$ at 230 GeV and $900 \pm 260 \text{ MeV}$ at 350 GeV.

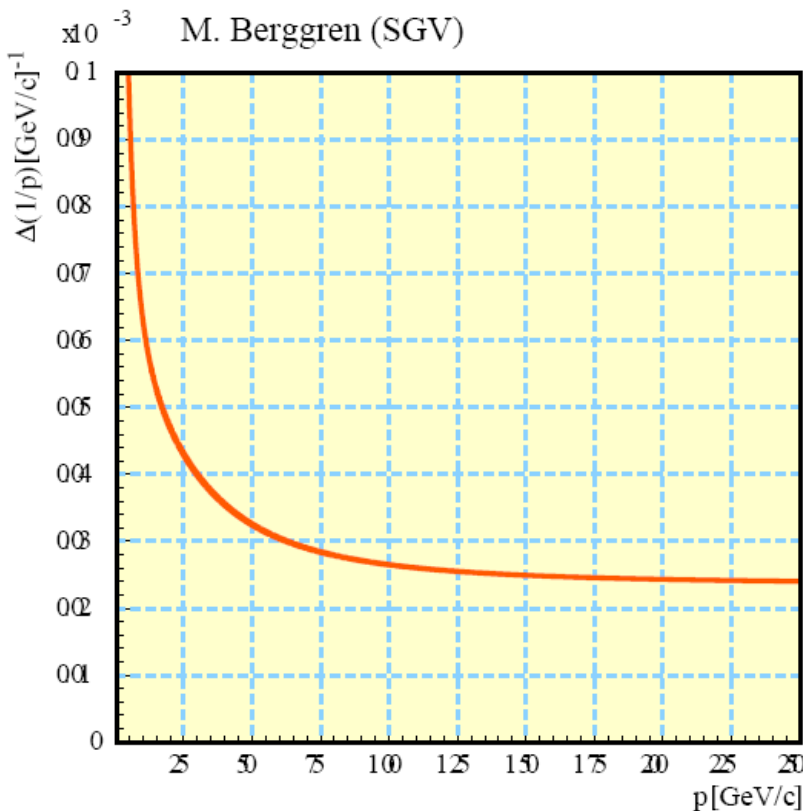


Figure 6: Momentum resolution for the LDC [10] detector concept with improved accuracies from the TPC and external silicon detectors.

2/ For hadronic decays of the Z boson one can use a kinematic fit with one constraint, imposing that:

$$M_Z^2 = 2pp'(1 - \cos \vartheta)$$

With this constraint and neglecting the angular errors and the Z width one has:

$$\delta M_h^2 = 4EA\sqrt{p}\left(1 - \frac{p'}{p}\right)$$

where the calorimeter accuracy is $dp=A\sqrt{p}$ with $A \sim 0.3$. Again, the largest errors come from asymmetric decays. To minimize this error one should determine p , the highest momentum, from calorimetry and deduce p' from the 1C constrain. Near threshold, $p \sim p'$ and therefore the above error becomes very small.

There is an additional error due to the Z natural width:

$$\delta M_h^2 = \frac{\delta M_Z^2}{M_Z^2} (M_Z^2 - 4Ep)$$

Recall that this effect has to be linearly added to the preceding term with the empirical formula given in the main text:

$$\sigma = \sigma^0 + 0.65 * \Gamma / 2$$

At 230 GeV, one finds an averaged mass resolution of 2.3 ± 0.8 GeV (the variation corresponds to the spread in momentum of the quarks). At 350 GeV, the same calculation gives a resolution of 7.3 ± 2.3 GeV. Note that in the latter case one needs to measure jets energies up to 150 GeV which may be challenging for the particle flow method [11]. We have nevertheless kept the same coefficient $A=0.3$ in the whole momentum range.

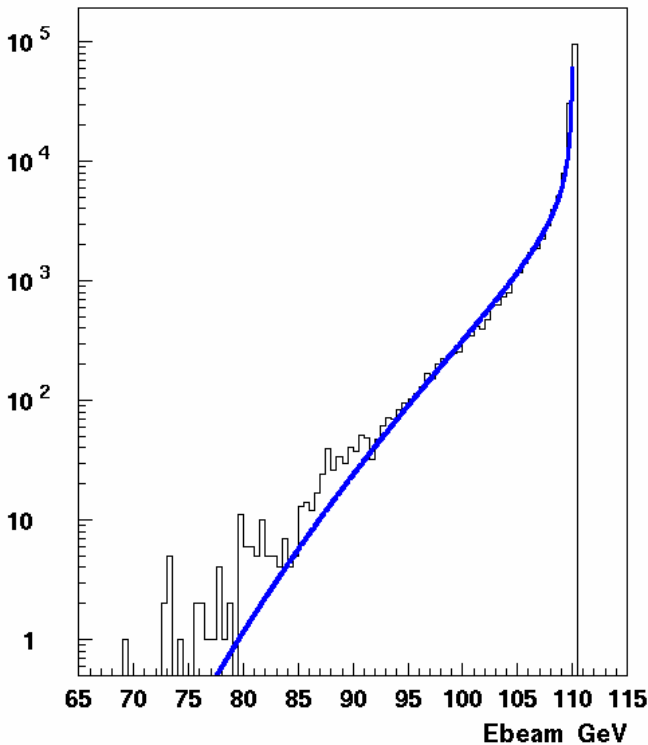


Figure 7: Differential spectrum for interacting beam particles computed with the Guinea-Pig simulation [4] and analytically using the expressions in [3].

3/ For Z and Higgs hadronic final states, one can perform a 5C fit which gives $\sim 2.5(2)$ GeV mass resolution on the Higgs mass, at 350(230) GeV centre of mass energy.

Radiative effects

There are four different radiative effects to be considered: beamstrahlung, ISR, FSR and external radiation for final state electrons.

1/ For beamstrahlung, we have cross-checked the P. Chen parameterisation in [3] with Guinea-Pig simulation [4] performed at $\sqrt{s}=220$ GeV. The agreement is reasonably good (see

2/ ISR and FSR can be simply described through the probability distribution:

$$dP = b \frac{dx}{x^{1-b}}$$

where $x=k/E$ is the ratio between the photon and the lepton energies and:

$$b = \frac{2\alpha}{\pi} [\log(\frac{M^2}{m^2}) - 1]$$

where m is the lepton mass and M is the lepton pair mass. For ISR one has simply $M^2=s$ and m is the electron mass. For FSR $M=M_Z$. Remarkably enough one cannot neglect muon FSR, for which $b=5.8\%$, with respect to electron FSR, for which $b=10.8\%$.

3/ External radiation is only relevant for electrons and is governed by the detector properties. For the purpose of this study we have assumed that an electron will see, on average, $d=3\%$ of X^0 before entering the TPC. We have then added this contribution to the FSR for the electrons, taking $b=2(4d/3X^0) = 8\%$ to account for both leptons. This figure shows that the detector properties amplify significantly the losses due to FSR. The net result, shown in Table 1, is a reduction in efficiency of a factor of about two for electrons with respect to muons.

In practice one should convolute the Gaussian (or Breit Wigner) shape of the mass resolution with the probability distribution. This gives for the radiation effect the following attenuation on the peak:

$$P = \left(\frac{\Gamma}{M}\right)^b = \left(\frac{2.35\sigma}{M}\right)^b$$

where $M=E_{cm}$ for ISR and $M=M_Z$ for FSR. This formula can be intuitively derived by integrating the probability distribution given above between 0 and $\Gamma/2$.

The $ZZ\gamma$ background

The ZZ process dominates the background to the HZ channel if one uses the recoil mass method with lepton pairs. In the absence of radiation, only ZZ^* can contaminate HZ with $M_{Z^*}=M_H$. This contribution is however typically one order of magnitude below the contribution from $ZZ\gamma$, where the photon comes either from ISR or from beamstrahlung. This process constitutes a significant background when the energy of this photon is such that one of the Z boson combinations peaks at the Higgs boson mass.

The various components of the ZZ background, for the two energies discussed in the paper, are given in Table 5. For what concerns this background one sees that reducing further the beamstrahlung would not help much near threshold.

Energy GeV	$ZZ^*(120)$	$ZZ\gamma$ RC	$ZZ\gamma$ BS	Sum fb/GeV
230	1	6.7	0.2	7.9
350	0.7	3.1	2.1	5.9

Table 5: Expected backgrounds for $HZ(120 \text{ GeV})$, in fb/GeV, coming from the ZZ process, at the two energies. The $ZZ^*(120)$ background gives a virtual Z at 120 GeV. In the other two processes there is a photon (from initial radiation or beamstrahlung) emitted in the beam pipe with two Z bosons on mass-shell such that the recoil mass to the Z decaying leptonically peaks at 120 GeV.